Investigation of the Exclusive ^3He(e,e′pn)^1H Reaction

Middleton, D. G.; Annand, J. R. M.; Antelo, M. Ases; Ayerbe, C.; Barneo, P.; Baumann, D.; Bermuth, J.; Bernauer, J.; Blok, H. P.; Bohm, R.; ...

Investigation of the Exclusive ^{3}He$(e, e'pn)^1$H Reaction

D. G. Middleton,[1,*] J. R. M. Annand,[2] M. Ases Antelo,[3] C. Ayerbe,[3] P. Barneo,[4] D. Baumann,[3] J. Bermuth,[3] J. Bernauer,[3] H. P. Blok,[4,5] R. Böhm,[3] D. Bosnar,[6] M. Ding,[3] M. O. Distler,[3] J. Friedrich,[3] J. García Llongo,[3] D. I. Glazier,[2] J. Golak,[7] W. Glöckle,[8] P. Grabmayr,[1] T. Hehl,[1] J. Heim,[1] W. H. A. Hesselink,[4,5] E. Jans,[4] H. Kamada,[9] G. Jover Mañas,[3] M. Kohl,[3] L. Lapikás,[4] I. J. D. MacGregor,[2] I. Martin,[1] J. C. McGeorge,[2] H. Merkel,[3] P. Merle,[3] K. Monstad,[2] F. Moschini,[1] U. Müller,[3] A. Nogga,[10] R. Pérez-Benito,[3] Th. Pospischil,[3] M. Potokar,[11] G. Rosner,[2] M. Seimetz,[3] R. Skibiński,[7] H. de Vries,[4] Th. Walcher,[3] D. P. Watts,[2] M. Weinriefer,[3] M. Weiss,[3] H. Witała,[7] and B. Zihlmann[4,5]

[1]*Kepler Centre for Astro and Particle Physics, Physikalisches Institut, Universität Tübingen, D-72076 Tübingen, Germany*
[2]*Department of Physics and Astronomy, University of Glasgow, Glasgow G12 8QQ, Scotland*
[3]*Institut für Kernphysik, Johannes Gutenberg-Universität Mainz, D-55099 Mainz, Germany*
[4]*Nikhef, P.O. Box 41882, 1009 DB Amsterdam, The Netherlands*
[5]*Department of Physics, VU-university, Amsterdam, The Netherlands*
[6]*Department of Physics, University of Zagreb, Zagreb, Croatia*
[7]*M. Smoluchowski Institute of Physics, Jagiellonian University, PL-30059 Kraków, Poland*
[8]*Institut für Theoretische Physik II, Ruhr-Universität Bochum, D-44780 Bochum, Germany*
[9]*Department of Physics, Faculty of Engineering, Kyushu Institute of Technology, Kitakyushu 804-8550, Japan*
[10]*Institute for Advanced Simulation, Institut für Kernphysik, and Jülich Center for Hadron Physics, Forschungszentrum Jülich, D-52425 Jülich, Germany*
[11]*Institute Jožef Stefan, University of Ljubljana, Ljubljana, Slovenia*

(Received 6 March 2009; published 7 October 2009)

Cross sections for the ^{3}He$(e, e'pn)^1$H reaction were measured for the first time at energy transfers of 220 and 270 MeV for several momentum transfers ranging from 300 to 450 MeV/c. Cross sections are presented as a function of the momentum of the recoil proton and the momentum transfer. Continuum Faddeev calculations using the Argonne $V18$ and Bonn-B nucleon-nucleon potentials overestimate the measured cross sections by a factor 5 at low recoil proton momentum with the discrepancy becoming smaller at higher recoil proton momentum.

DOI: 10.1103/PhysRevLett.103.152501 PACS numbers: 25.10.+s, 21.30.Fe, 21.45.−v, 25.30.Fj

The understanding of nucleon-nucleon (NN) interactions within the nucleus is of great importance for modern nuclear physics. These NN interactions induce correlations between the nucleons. They are characterized at short internucleon separations by a strong scalar repulsive component and at intermediate to large separations by an attractive part, caused mainly by the strong tensor component of the meson-exchange contribution. The use of electron-induced exclusive two-nucleon knockout reactions of the type $A(e, e'pN)A-2$ is a very direct method for the study of this correlated behavior within the nucleus. Because the scalar and tensor interactions act differently in isospin $T = 0$ and $T = 1$ states pp and pn knockout reactions probe predominantly the short-range and tensor components, respectively [1,2]. Recently measurements were made at Jefferson Laboratory to study pp and pn correlations in ^{12}C [3,4]. It was found that pn correlations are about 9 times more likely than pp correlations.

The use of ^{3}He for the study of NN correlations via $(e, e'pN)N$ reactions has advantages over other nuclei. The final state is a single nucleon in its ground state so detector resolution is not critical and reconstruction of the final state is straightforward. Furthermore theoretical models exist [5–7] that allow the break-up cross section to be calculated exactly, with the NN interactions between all three nucleons taken into account, but without explicit inclusion of three-nucleon forces (3BF). Such models calculate both the ^{3}He ground state and the three-nucleon continuum wave functions using realistic NN potentials which include a phenomenological description of the short range part of the interaction [8,9].

At electron energies of several hundred MeV the electron-induced two-nucleon knockout cross section is driven by several processes. The coupling of the virtual photon to one nucleon of a correlated pair via one-body hadronic currents can lead to the ejection of both nucleons from the nucleus. Interaction of the virtual photon with two-body hadronic currents, such as meson-exchange currents (MECs) or isobar currents (ICs), also contributes to the cross section and interaction with all three nucleons [10] could also play a role. There can also be interactions between all particles in the final state (FSI), the strength of which depends strongly on the relative NN energies. In order to disentangle these different contributing processes it is important to measure both the $(e, e'pp)$ and $(e, e'pn)$ cross sections as a function of several kinematic variables.

Results from measurements of the ^{3}He$(e, e'pp)n$ reaction are reported in [11–13]. Here we present the results of a measurement of the ^{3}He$(e, e'pn)^1$H reaction.

The measurements were performed at the electron scattering facility of the 100% duty factor Mainz Microtron MAMI [14,15]. The 855 MeV electron beam, with currents between 2 and 4 μA, was incident on a ^{3}He high-pressure cryogenic gas target, operated at 1.9 MPa and 15 K. At 4 μA beam current this corresponds to a luminosity of 2×10^{36} cm^{-2} s^{-1}. The scattered electrons were detected in Spectrometer B [16], a magnetic spectrometer with a solid angle of $\Delta\Omega = 5.6$ msr and momentum acceptance of $\Delta p/p = 15\%$. The ejected protons were detected using the scintillator detector HADRON3 (H3) [17] from Nikhef, a large solid angle ($\Delta\Omega = 230$ msr) hodoscope with a proton energy acceptance of 50–250 MeV. For detection of the ejected neutrons the Glasgow-Tübingen time-of-flight (TOF) detector system [18] was used in a configuration similar to that described in [19]. The TOF array covered a solid angle of $\Delta\Omega \approx 240$ msr. After software cuts the neutron energy threshold in TOF was 16.7 MeV, while the use of 0.5 cm thick lead shielding in front of H3 resulted in an effective proton energy threshold of 70 MeV. Kinematics (see Table I) were chosen so that the reaction could be studied at energy and momentum transfers similar to those covered previously in a measurement of the ^{3}He$(e, epp)n$ reaction [12].

With the detection of two ejected nucleons from the initial $3N$ system, the kinematics of the reaction are completely determined. The missing momentum is defined as $\vec{p}_m = \vec{q} - \vec{p}_{p'} - \vec{p}_{n'}$ and is equal to the momentum of the undetected proton, $\vec{p}_r$; here $\vec{q}$ is the momentum transfer and $\vec{p}_{p'}$ and $\vec{p}_{n'}$ are the momenta of the detected proton and neutron, respectively. Using $\vec{p}_m$, the missing energy, $E_m = \omega - T_{p'} - T_{n'} - T_{r'}$, can be determined where ω is the energy transfer of the virtual photon and $T_{p'}$, $T_{n'}$ and $T_{r'}$ are the kinetic energies of the proton, neutron and undetected proton, respectively.

The missing-energy spectrum for the Z2 kinematic setting is shown in Fig. 1. The inset of Fig. 1 shows the missing-energy spectrum before the subtraction of accidental coincidences as well as the spectra for the different types of accidental coincidences. The $(e'p)$ and $(e'n) + (pn)$ types of accidental coincidences (red dashed and blue dotted curves) were subtracted from the total coincidence yield (black curve). As this subtracts the "e', p, n accidental" coincidences twice (green dot-dashed curve) these were added to the result to obtain the number of real coincident events. More details of the accidental subtraction procedure can be found in [19].

The missing-energy spectrum corrected for accidental coincidences has a single peak which corresponds to the three-body breakup of ^{3}He. The peak has a FWHM of 7.0 MeV, as expected from the known detector resolutions in energy and angle, and a mean value of 6.2 MeV, close to the expected value of 7.72 MeV. The tail at higher missing energies is due to radiative processes.

The eightfold differential cross section for the ^{3}He$(e, e'pn)$ reaction can be written as a fivefold differential cross section, $d^5\sigma/dSd\Omega_p d\Omega_n$, containing the nuclear structure information, multiplied by a virtual-photon flux factor Γ_v [20]. The cross section is differential in S, where dS is the arclength in the $T_{p'} - T_{n'}$ plane along the curve S that describes the relation between $T_{p'}$ and $T_{n'}$ for a given proton-neutron angular configuration [21,22]. It depends on seven independent kinematic variables, but due to the limited statistics of the data, it will be presented as function of one of them only, integrating over the others within the acceptance of the detectors. The average fivefold experimental cross section was calculated as:

$$\frac{d^5\sigma}{dSd\Omega_p d\Omega_n}(x) = \frac{1}{\int \mathcal{L}dt}\frac{N(x, \Delta x)}{\mathcal{V}(x, \Delta x)} \quad (1)$$

where Δx represents a range (bin) in the variable x as a function of which the cross section is presented, $\int \mathcal{L}dt$ is the integrated luminosity, $N(x, \Delta x)$ is the measured number of $(e, e'pn)$ events in bin Δx, corrected for accidental coincidences, integrated over the missing-energy range from below the peak up to 36 MeV, and $\mathcal{V}(x, \Delta x)$ is the corresponding phase-space element. The latter was determined by a Monte Carlo method using 10^8 events, generated within the energy or momentum acceptances of the three detectors involved, taking into account energy conservation for the reaction. Radiative corrections were applied to the phase space which were calculated using the formalism of Mo and Tsai [23]. The factor Γ_v was also included as a weight, as were the efficiencies of the H3 and TOF detectors. The former ranged from 90% to 80% depending on the proton energy. The neutron detection

TABLE I. Kinematic settings in which the data were taken. The detector angles given are the central angle of each detector in the lab frame; three stands of TOF detectors were used.

Label	ω [MeV]	q [MeV/c]	θ_B [deg]	θ_{H3} [deg]	θ_{TOF} [deg]			θ_q [deg]
A1	220	375	23.8	−53.3	107.7	125.5	140.5	−43.1
A2	270	375	20.9	−44.0	107.7	125.5	140.5	−34.3
B2	270	450	29.3	−44.0	107.7	125.5	140.5	−39.8
Y1	220	300	15.4	−45.0	107.7	125.5	140.5	−35.5
Z2	270	330	15.9	−45.0	107.7	125.5	140.5	−28.1

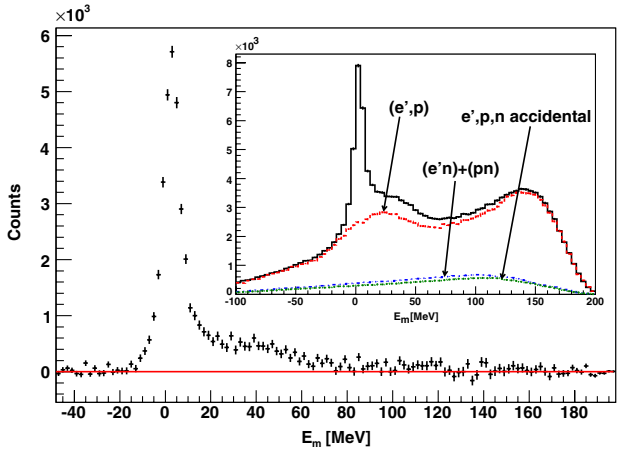

FIG. 1 (color online). The missing-energy (E_m) distribution for the ^{3}He($e, e'pn$) reaction for the Z2 kinematic setting. The inset shows the E_m distribution before subtraction of accidental coincidences. See the text for details on the curves.

efficiency was about 8% on average for the signal pulse-height threshold applied in the analysis. It was computed with a model based on the Stanton code [24,25] which agreed to within 10% with measurements made for 30–60 MeV neutrons using a ^{2}H target. Finally the phase space was integrated over the missing energy to yield $\mathcal{V}(x, \Delta x)$ using the same limits as in the determination of $N(x, \Delta x)$, and over all variables except x, applying the same cuts in $T_{p'}$ and $T_{n'}$ as for the experimental data. The statistical error associated with the generated phase space is $\leq 0.5\%$. Corrections for dead time in the electronics were included in the determination of the integrated luminosity $\int \mathcal{L} dt$.

In the figures only the statistical errors are shown. The overall systematic error is about 13% with the largest contribution coming from the uncertainty ($\approx$12%) in the neutron detection efficiency. The uncertainty in the correction for hadronic interactions and multiple scattering in H3 is about 4%. Other contributions to the systematic error such as those from luminosity calibration, dead time corrections and target-thickness determination from elastic scattering, are negligible compared to those of the detection efficiency corrections.

The measured cross sections are compared to the results of nonrelativistic continuum Faddeev calculations [6] using the Argonne $V18$ ($AV18$) and Bonn-B (BB) NN potentials. The calculations contain mechanisms for photon absorption on one or two of the nucleons in the target nucleus but are limited in their treatment of MEC, IC and 3BF which might be important at the considered kinematics. The calculations are only strictly applicable for photon energies below pion production threshold. Rescattering processes up to all orders in the continuum are included ensuring that all FSI effects are fully taken into account. Two types of calculations were made. The first employed only a one-body hadronic current operator, while the second also included a two-body current operator for π and ρ mesons to account for the in-flight and seagull terms using the formalism of Schiavilla *et al.* [26] which is based on earlier work of Riska [27,28].

The calculation of the theoretical cross sections was done in two steps. In the first part the Faddeev equations were solved for a single, central (ω, q) point per kinematic setting. All NN-force components were included up to a two-body angular momentum of $j = 3$ and in the final state all partial waves were included up to three-body angular momentum $J = \frac{15}{2}$. Then the cross section was calculated for many specific three-nucleon final states determined by $\vec{p}_{p'}$ and $\vec{p}_{n'}$ for a given (ω, q) point. The final states were randomly generated over the full acceptance of the H3 and TOF detectors using a generator similar to that used for the phase space. Approximately 10^7 events were generated for each (ω, q) point to ensure full coverage and to reduce statistical fluctuations. The average calculated cross section for each (ω, q) point was used for comparison with the experimental data.

The effect of using only the central (ω, q) point was investigated for one kinematic setting. The average difference in the calculated theoretical cross section between using just the central value or using a range covering the whole acceptance of spectrometer B was found to be about 10%.

Figure 2 shows the ^{3}He($e, e'pn$) cross section as a function of the missing momentum for the A1 kinematic setting. The overall shape of the measured and theoretical cross sections is similar in that they decrease roughly exponentially with increasing p_m. The inclusion of MECs increases the calculated cross section by only about 10% up to $p_m = 200$ MeV/c but the effect increases to about 60% at 350 MeV/c. The use of the two different potentials makes little difference to the results of the calculations which overpredict the experimental data by

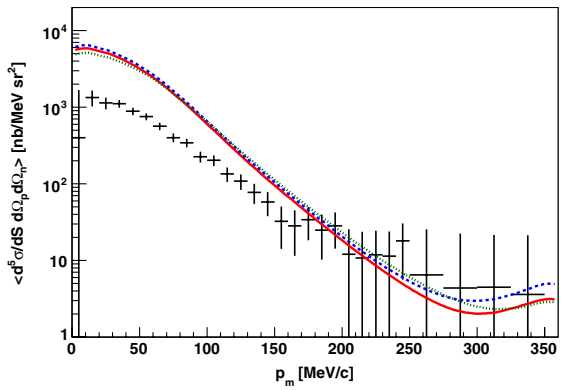

FIG. 2 (color online). The ^{3}He($e, e'pn$) reaction cross section, averaged over the experimental acceptance, as a function of the missing momentum for the A1 kinematic setting. The solid red (dotted green) curve shows the theoretical cross section calculated using only a one-body hadronic current operator and the $AV18$ (BB) NN potential. The dashed blue line results from the $AV18$ potential when MECs are also included.

about a factor of 5 for $p_m \leq 80$ MeV/c. The discrepancy decreases with increasing p_m until rough agreement within the large experimental error bars is reached at $p_m \approx 200$ MeV/c. The calculations indicate that for the kinematics shown here the ^{3}He($e, e'pn$) cross section is dominated by the one-body hadronic current term.

The overprediction of the cross section by the theoretical calculations is in contrast to the ^{3}He($e, e'pp$) reaction [12] where calculations using the BB potential are slightly below the data at low p_m and a factor of 5 lower at $p_m = 200$ MeV/c. There is not only a clear difference in the ratio between the pp and pn-knockout data and their respective one-body current prediction, but also both measured cross sections do not fall as quickly as predicted with increasing p_m.

This different behavior between pp and pn knockout is intriguing. The large discrepancy at low p_m in the case of pn knockout, where the virtual photon supposedly couples mainly to one of the nucleons of a pn pair, would suggest that the pn correlations in the probed regime are not well predicted by the theory. Other sources of disagreement could be the effect of 3BF, which are not included in the theoretical model, or the incomplete treatment of MECs and the omission of ICs, which play a much larger role in pn than in pp knockout.

Figure 3 shows the ^{3}He($e, e'pn$) cross section as a function of q for the ranges $235 \leq \omega \leq 265$ MeV and $50 \leq p_m \leq 100$ MeV/c where effects due to 3BF might be expected to be small. The experimental cross section shows a smoothly rising q dependence which increases by about a factor 2 from $q = 300$ to 450 MeV/c. The theoretical calculations overpredict the measured cross sections by a factor 2–3 at $q = 320$ MeV/c to a factor of about 5 at $q = 450$ MeV/c. The inclusion of MECs increases the calculated cross section by about 30% at $q = 320$ MeV/c. This increase falls with increasing q to about 5% at $q = 450$ MeV/c.

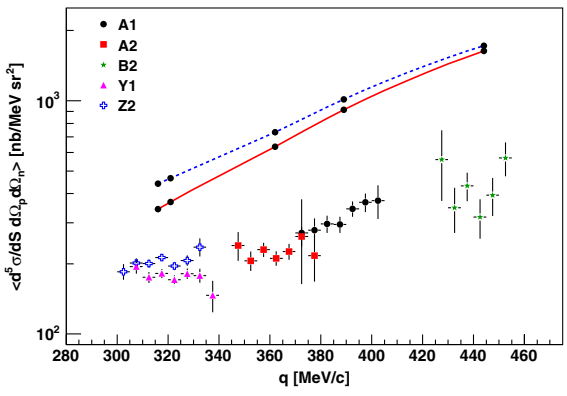

FIG. 3 (color online). The ^{3}He($e, e'pn$) reaction cross section shown as a function of q for $50 \leq p_m \leq 100$ MeV/c and $235 \leq \omega \leq 265$ MeV. Results from different kinematic settings are shown by the different types of markers for the data points. The line convention is the same as in Fig. 2. The theoretical cross section was calculated at the points indicated by the black circles.

The q dependence of the ^{3}He($e, e'pp$) data for a similar p_m range is much better described by the calculations with just a q-independent underprediction of 20%. Again this points to an inadequacy in the theoretical calculations for pn knockout, as discussed above.

In conclusion the ^{3}He($e, e'pn$) reaction was measured with good statistical accuracy over a range of momentum transfers and for two energy transfers. Calculations using the $AV18$ or BB potentials overpredict the measured cross sections by a factor 5 at low p_m but are in rough agreement within the large statistical experimental errors at $p_m \geq 200$ MeV/c. Inclusion of MECs increases the calculated cross section by about 10% up to $p_m = 200$ MeV/c, increasing to about 60% at $p_m = 350$ MeV/c. When the cross section at low p_m is considered as a function of q the calculations overpredict the data by a factor 2 to 5.

Comparison with data measured for the ^{3}He($e, e'pp$) reaction, which are much better described by the same theoretical calculations at low p_m, suggests that the pn correlations in the probed kinematical regime are not well described and/or reaction mechanisms that are not included in the calculations (such as IC, certain MECs and 3BF) play an important role. The good statistical accuracy of the reported measurements together with the striking disagreement with current theoretical models will hopefully encourage further theoretical work.

The authors would like to thank the staff of the Institut für Kernphysik in Mainz for providing the facilities for this experiment. This work was sponsored by the UK Science and Technology Facilities Council (STFC), the Deutsche Forschungsgemeinschaft (DFG) and the Foundation for Fundamental Research of Matter (FOM), which is financially supported by the Netherlands Organization for Scientific Research (NWO). It was also partially supported by the 2008–2011 Polish Science Funds as research Project No. NN202 077435. The numerical calculations were performed at the NIC, Jülich, Germany.

*duncan@pit.physik.uni-tuebingen.de

[1] R. Schiavilla, R. B. Wiringa, S. C. Pieper, and J. Carlson, Phys. Rev. Lett. **98**, 132501 (2007).
[2] R. B. Wiringa, R. Schiavilla, S. C. Pieper, and J. Carlson, Phys. Rev. C **78**, 021001(R) (2008).
[3] R. Shneor *et al.*, Phys. Rev. Lett. **99**, 072501 (2007).
[4] R. Subedi *et al.*, Science **320**, 1476 (2008).
[5] E. van Meijgaard and J. A. Tjon, Phys. Rev. C **45**, 1463 (1992).
[6] J. Golak, R. Skibiński, H. Witała, W. Glöckle, A. Nogga, and H. Kamada, Phys. Rep. **415**, 89 (2005).
[7] A. Deltuva, L. P. Yuan, J. Adam, and P. U. Sauer, Phys. Rev. C **70**, 034004 (2004).
[8] J. Carlson and R. Schiavilla, Rev. Mod. Phys. **70**, 743 (1998).

[9] A. Nogga, H. Kamada, W. Glöckle, and B. R. Barrett, Phys. Rev. C **65**, 054003 (2002).
[10] St. Kistryn *et al.*, Phys. Rev. C **68**, 054004 (2003).
[11] D. L. Groep *et al.*, Phys. Rev. Lett. **83**, 5443 (1999).
[12] D. L. Groep *et al.*, Phys. Rev. C **63**, 014005 (2000).
[13] R. A. Niyazov *et al.*, Phys. Rev. Lett. **92**, 052303 (2004).
[14] H. Herminghaus *et al.*, Nucl. Instrum. Methods Phys. Res., Sect. A **138**, 1 (1976).
[15] Th. Walcher, Prog. Part. Nucl. Phys. **24**, 189 (1990).
[16] K. I. Blomqvist *et al.*, Nucl. Instrum. Methods Phys. Res., Sect. A, **403**, 263 (1998).
[17] A. Pellegrino *et al.*, Nucl. Instrum. Methods Phys. Res., Sect. A **437**, 188 (1999).
[18] P. Grabmayr *et al.*, Nucl. Instrum. Methods Phys. Res., Sect. A **402**, 85 (1998).
[19] D. G. Middleton *et al.*, Eur. Phys. J. A **29**, 261 (2006).
[20] F. Halzen and A. D. Martin, *Quarks and Leptons* (J. Wiley and Sons, New York, 1984).
[21] J. Golak, H. Kamada, H. Witała, W. Glöckle, and S. Ishikawa, Phys. Rev. C **51**, 1638 (1995).
[22] G. G. Ohlsen, Nucl. Instrum. Methods **37**, 240 (1965).
[23] L. Mo and Y. Tsai, Rev. Mod. Phys. **41**, 205 (1969).
[24] R. M. Edelstein *et al.*, Nucl. Instrum. Methods **100**, 355 (1972).
[25] R. A. Cecil *et al.*, Nucl. Instrum. Methods **161**, 439 (1979).
[26] R. Schiavilla, V. R. Pandharipande, and D. O. Riska, Phys. Rev. C **40**, 2294 (1989).
[27] D. O. Riska, Phys. Scr. **31**, 107 (1985).
[28] D. O. Riska, Phys. Scr. **31**, 471 (1985).